PAPER

Promoting and inhibiting tunneling *via* nuclear motions†

Attila G. Császár* and Tibor Furtenbacher

Accurate, experimental rotational–vibrational energy levels determined *via* the MARVEL (Measured Active Rotational–Vibrational Energy Levels) algorithm and published recently for the symmetric-top $^{14}NH_3$ molecule in *J. Quant. Spectrosc. Radiat. Transfer*, 2015, **116**, 117–130 are analyzed to unravel the promoting and inhibiting effects of vibrations and rotations on the tunneling splittings of the corresponding symmetric (s) and antisymmetric (a) rovibrational energy level pairs. The experimental transition data useful from the point of view of the present analysis cover the range 0.7–7000 cm^{-1}, sufficiently detailed rovibrational energy sets worth analyzing are available for 20 vibrational bands. The highest J value, where J stands for the rotational quantum number, within the experimental dataset employed is 30. Coupling of the "umbrella" motion of $^{14}NH_3$ with other vibrational degrees of freedom has only a minor effect on the a–s tunneling splitting characterizing the ground vibrational state, 0.79436(70) cm^{-1}. In the majority of the cases rotation around the C_3 axis increases, while rotation around the two perpendicular axes decreases the tunneling splittings. For example, for the pair of vibrational ground states, 0^+ and 0^-, the tunneling splitting basically disappears at around $J = 25$ for the $(J,K) = (J,1)$ states, where $K = |k|$ is the usual quantum number characterizing the projection of the rotational angular momentum on the principal axis. The tunneling splittings, defined as energy differences $E(a) - E(s)$ of corresponding energy level pairs, as a function of J and K show a very regular behavior for the ground state (GS) and the $n\nu_2$ bands. For the other bands investigated exceptions from a regular behavior do occur, especially for bands characterized by degenerate vibrations, and occasionally the data available are not sufficient to arrive at definitive conclusions. The most irregular behavior is observed for rotational states characterized by the $k - l = 3n$ rule (l is the vibrational angular momentum quantum number), with $n = 0, 1, 2,...$ High-quality, variationally computed rovibrational data support all the conclusions of this study based on experimental energy levels.

1 Introduction

The ammonia molecule has been playing a vital role in the development of spectroscopy and the quantum theory needed to understand measured spectral features. The first measurement of the spectrum of ammonia dates back prior to 1905.[1] Several further measurements, and their interpretations, followed in the 1920s,[2–11] 1930s,[12–23] and 1940s.[24–35] A large number of the later experimental studies are nicely summarized and reviewed in ref. 36.

Following detailed pioneering studies in 1926[3] and 1928,[4–6] 1929 was a particularly fruitful year concerning the molecular spectroscopy of ammonia. Dickinson *et al.*[9] observed both vibrational and rotational transitions in the first Raman spectrum recorded for NH$_3$. In the same year, Barker[8,10] employed the double-well potential to explain the experimentally observed double character of the band at 10 μ.

In 1932, Dennison and Hardy "searched for the doubling of the 3 μ band using an infrared spectrometer of high resolving power".[13] Dennison continued to play[23,25,31] a vital role in the theoretical understanding of the spectroscopy and in particular the inversion/tunneling dynamics of ammonia.

As borne out in these pioneering studies, the quantum chemical model of the ammonia molecule involves a large-amplitude vibrational motion called inversion, characterized by a symmetric double-well potential.[14,21,23,25,27,28,31,37–41] The height of the one-dimensional electronic barrier is 1773 ± 13 cm^{-1}, increasing to 2021 ± 20 cm^{-1} when the effect of zero-point vibrations is considered.[38,41–44] Treating the inversion motion is challenging for perturbative approaches and calls for fourth-age quantum chemical[45] nuclear motion treatments.[44,46–52] Note that the vibration–rotation tunneling dynamics of partially or fully deuterated ammonia species has also been subjected to detailed experimental and quantum chemical studies.[44,53–55]

Institute of Chemistry, Loránd Eötvös University, Pázmány sétány 1/A, Hungary and MTA-ELTE Complex Chemical Systems Research Group, H-1518 Budapest 112, P. O. Box 32, H-1117 Budapest, Hungary. E-mail: csaszar@chem.elte.hu
† Electronic supplementary information (ESI) available. See DOI: 10.1039/c5cp04270d

Promoters (catalyzers) and inhibitors change the shape, in particular the height and the width, of the effective barrier hindering a reaction. Tunneling can be viewed as a chemical reaction and it is extremely sensitive to small local details of the potential energy surface (PES), as proven by many interesting phenomena related to it.[56] As investigated explicitly here and implicitly before,[52,57] nuclear motions, vibrations and rotations, can have a significant effect on the effective tunneling barrier and consequently the tunneling splittings characterizing ammonia. Nuclear motion effects can be monitored very sensitively by the tunneling splittings of the corresponding symmetric (s) and antisymmetric (a) energy levels. It is our hope that the conclusions of this study with respect to the vibration–rotation tunneling dynamics of $^{14}NH_3$ will prove to be useful for a wider range of chemical systems and even for true chemical reactions.

2 MARVEL energy levels

A recent publication[36] reported the results of a MARVEL analysis of the close to 30 000 measured transitions of $^{14}NH_3$, where MARVEL stands for measured active rotational–vibrational energy levels.[58–62] The vibrational MARVEL energy levels employed in this study are given in Table 1. Since the experimental-quality MARVEL energy levels form the basis of the present investigation, a couple of related points need to be discussed. For further details the reader is referred to ref. 36.

$^{14}NH_3$ is a pyramidal molecule corresponding to the molecular symmetry (MS) group $D_{3h}(M)$.[63] (Ro)vibrational states with symmetry $A_1^{\dagger} := \{A_1', A_1''\}$ are not allowed ('missing') due to their zero nuclear spin statistical weight factors. Formally, $A_1^{\dagger}$ states are involved in tunneling splittings characterizing the rovibrational energy level structure of $^{14}NH_3$ making the spectroscopic analysis more complex and less complete as some vibrational tunneling splittings cannot be determined experimentally.

Next, recall what 9 of the 12 descriptors labelling the MARVEL rotation–vibration levels of NH_3,[36] (v_1 v_2 v_3 v_4 l_3 l_4 J K i), mean. The vibrational labels employ the normal-mode notation, (v_1 v_2 v_3 v_4 l_3 l_4), where the corresponding v_1 and v_2 are the symmetric stretch and symmetric bend modes, respectively, and l_3 and l_4 are vibrational angular momentum quantum numbers corresponding to the doubly degenerate v_3 (antisymmetric stretch) and v_4 (antisymmetric bend) modes, respectively. Naturally, $l_m = -v_m, -v_m + 2, \ldots, v_m - 2, v_m$ with $m = 3, 4$ (later on, the notation $v_m^{l_m}$ will sometimes be used). Furthermore, $l = l_3 + l_4$, where l represents the total vibrational angular momentum. Following ref. 64, $L_3 = |l_3|$, $L_4 = |l_4|$, and $L = |l|$.

$^{14}NH_3$ is a symmetric-top rotor. Rotations are described by the rigorous quantum number J and the quantum number K (and $K = |k|$) corresponding to the projection of the rotational angular momentum **J** on the C_3 symmetry axis, $k = -J, \ldots, J$. The next descriptor, i, corresponds to the inversion symmetry of the v_2 vibrational motion, which can take values of 0 or 1 (symmetric, s, or antisymmetric, a, respectively, with respect to reflection in the inversion plane) and this descriptor is central

Table 1 MARVEL vibrational band origins (VBOs) for $^{14}NH_3$, determined in ref. 36, with standard abbreviated (SA) and detailed normal-mode (v_1 v_2 v_3 v_4 L_3 L_4 L) labels, vibrational symmetries (Γ_v) corresponding to the molecular symmetry group $D_{3h}(M)$, and MARVEL uncertainties (Unc.)[a]

SA	v_1	v_2	v_3	v_4	L_3	L_4	L	Γ_v	VBO/cm^{-1}	Unc.[a]
0^+	0	0	0	0	0	0	0	A_1'	0.000000[b]	0[b]
0^-	0	0	0	0	0	0	0	A_2''	0.794368	697
v_2^-	0	1	0	0	0	0	0	A_2''	968.122894	497
v_4^+	0	0	0	1	0	1	1	E'	1626.274636	1544
v_4^-	0	0	0	1	0	1	1	E''	1627.372362	2168
$2v_2^-$	0	2	0	0	0	0	0	A_2''	1882.178422	1152
$(v_2 + v_4)^+$	0	1	0	1	0	1	1	E'	2540.523012	1411
$(v_2 + v_4)^-$	0	1	0	1	0	1	1	E''	2586.126091	1980
$3v_2^-$	0	3	0	0	0	0	0	A_2''	2895.522916	1411
$2v_4^{0,-}$	0	0	0	2	0	0	0	A_2''	3217.588264	1782
$2v_4^{2,+}$	0	0	0	2	0	2	2	E'	3240.162903	3086
$2v_4^{2,-}$	0	0	0	2	0	2	2	E''	3241.598311	1782
v_1^-	1	0	0	0	0	0	0	A_2''	3337.097887	3651
v_3^+	0	0	1	0	1	0	1	E'	3443.628071	968
v_3^-	0	0	1	0	1	0	1	E''	3443.987642	968
$(v_1 + v_2)^-$	1	1	0	0	0	0	0	A_2''	4320.031622	2080
$(v_2 + v_3)^+$	0	1	1	0	1	0	1	E'	4416.915038	1000
$(v_2 + v_3)^-$	0	1	1	0	1	0	1	E''	4435.446463	2000
$(v_1 + v_4)^+$	1	0	0	1	0	1	1	E'	4955.756078	1000
$(v_1 + 2v_4^2)^+$	1	0	0	2	0	2	2	E'	6556.421597	1988
$(v_1 + 2v_4^2)^-$	1	0	0	2	0	2	2	E''	6557.930442	5185
$(v_1 + v_3)^+$	1	0	1	0	1	0	1	E'	6608.821870	1988
$(v_1 + v_3)^-$	1	0	1	0	1	0	1	E''	6609.753328	2478
$(v_3 + 2v_4^2)^+$	0	0	1	2	1	2	1	E'	6677.431678	1990
$(v_3 + 2v_4^2)^-$	0	0	1	2	1	2	1	E''	6678.310343	1990
$(v_2 + 3v_4^1)^-$	0	2	0	3	0	1	1	E''	6678.929943	2000
$2v_3^{2,+}$	0	0	2	0	2	0	2	E'	6850.244878	5300
$2v_3^{2,-}$	0	0	2	0	2	0	2	E''	6850.654943	3900

[a] The VBOs are reported in the order of increasing energy. The uncertainties are given in units of 10^{-6} cm^{-1}. 0 corresponds to the vibrational ground state, sometimes also referred to as GS. [b] The value of the vibrational ground state is fixed to zero with zero uncertainty.

to the present study. In what follows, these descriptors are sometimes grouped as $[J K i]$.

During the present investigation, a few problems have been realized and corrected concerning the original set of transitions treated and the energy levels reported in ref. 36. These are described in the Electronic Supplementary Material (ESM) and resulted in the removal of 57 energy levels and the transitions determining them (Table S1, ESI†), as well as in the relabeling of 56 transitions (Table S2, ESI†). The remaining energy levels in the region of 0.7–7000 cm^{-1} have been utilized for this study.

3 Tunneling splittings affected by vibrational motions

Fig. 1 presents an overview of those vibrational band origins (VBOs) and related tunneling splittings of $^{14}NH_3$ which have been established in ref. 36. Despite the fact that a large number of rovibrational transitions have been measured for $^{14}NH_3$, there are only 30 VBOs, eight for *ortho-* and 22 for *para-*$^{14}NH_3$, determined experimentally for this molecule.[36] Two *para-*$^{14}NH_3$ VBOs fall outside the range of interest of this study, 0–7000 cm^{-1}. Direct determination of rotationless ($J = 0$) VBOs of $A_1^{\dagger}$

This journal is © the Owner Societies 2016

Phys. Chem. Chem. Phys., 2016, **18**, 1092–1104 | 1093

Fig. 1 Energies and related tunneling splittings for all the MARVEL vibrational band origins (VBO)[36] of $^{14}NH_3$ under 7000 cm^{-1}. The green and red colors mean VBOs of *ortho*- and *para*-$^{14}NH_3$, respectively, while black means that the level has not been or could not be determined experimentally. For all measured tunneling splittings uncertainties are explicitly provided, for unmeasured splittings only one digit after the decimal place is given. The separation of the split energy levels mostly had to be distorted for easier reading.

symmetry is impossible. The experimental (MARVEL) coverage of VBOs is complete only up to 3500 cm^{-1}, the first missing VBO, of E'' symmetry, is at 3502 cm^{-1}.[36] The uncertainties of the measured VBOs are fairly substantial, usually on the order of 0.001–0.004 cm^{-1}.

If one of the energy levels involved in the tunneling splittings cannot be measured (a "missing" level by symmetry), see Fig. 1 with VBOs color coded based on their symmetry, we cannot obtain the related $E(a) - E(s)$ difference with the usual experimental accuracy. To indicate this problem, in Fig. 1

uncertainties are explicitly given when both levels involved in the splitting are available from experiments and no uncertainty is given when at least one of the levels has not been determined (or impossible to determine) experimentally.

The most famous tunneling splitting of ammonia is that of the "ground" vibrational state and the experimentally determined MARVEL $E(a) - E(s)$ value is 0.79436(70) cm^{-1}.[36] Although the lower energy level involved in this splitting is a "missing" level, since its energy is set to zero by definition this energy difference can be considered to be determined

1094 | *Phys. Chem. Chem. Phys.*, 2016, **18**, 1092–1104

This journal is © the Owner Societies 2016

experimentally. Note that this tunneling splitting appeared in the 1940 review article of Dennison[24] about ammonia spectroscopy as 0.66 cm^{-1}, reasonably close to its present-day value.

Tunneling splittings characterizing the vibrational fundamentals of $^{14}NH_3$ are as follows. Since the ν_1^+ state is of A_1' symmetry, it can only be estimated, based on accurate variational computations[51,52] and effective Hamiltonians, that the tunneling splitting is about 1.0 cm^{-1} for this fundamental. Similarly, the tunneling splitting of ν_2 can be determined only approximately: it is about 35.7 cm^{-1}. The experimental tunneling splitting characterizing ν_3 is 0.3596(14) cm^{-1}, while that of ν_4 is 1.0977(27) cm^{-1}.

It is clear that once the energy of the VBO approaches the height of the effective tunneling barrier, the energy deficiency to bypass the tunneling barrier becomes smaller and the tunneling path becomes shorter; thus, the tunneling splitting has to increase. This is most relevant, of course, for the ν_2 fundamental and its overtones. As noted, the splitting characterizing the ν_2 fundamental is large, 35.7 cm^{-1}, about 40 times larger than that of the "ground" vibrational state (or of the other fundamentals). Divergence of the tunneling splittings characterizing the ν_2 overtones is fast and, as well known, the "umbrella" states above the barrier retain, to a considerable degree, the motion characteristics. The approximate measured splittings of $2\nu_2$, still below the barrier, and $3\nu_2$ are 282 and 511 cm^{-1}, respectively. No further $n\nu_2$ overtone splittings have been measured experimentally. Nevertheless, these are known from accurate variational nuclear motion computations, the ref. 51 (ref. 52) data indicate that the splittings of $4\nu_2$, $5\nu_2$, $6\nu_2$, and $7\nu_2$ are 599.7(599.3), 665.1(665.5), 708.1(707.0), and 747.5(744.1) cm^{-1}, respectively. Thus, their magnitude slowly increases while their separation slowly decreases as the level of excitation increases.

The effect of the other types of vibrational motions on tunneling splittings can be investigated by studying the combination levels, most importantly the $\nu_2 + \nu_i$, $i = 1, 2, 3, 4$, combinations.

Symmetric stretching of the N–H bonds, when mixed with the umbrella motion, results in a quenching of the splitting, from 35.7 to 25.5 cm^{-1} (the non-degenerate $\nu_1 + \nu_2$ combination band of ammonia, see Fig. 1). Thus, moving the hydrogens

further from each other results, through a motion which is symmetrically allowed to mix with the umbrella motion, in an increase of the effective barrier height and, perhaps more importantly, an increase in the length of the tunneling path. Recent experimental results[65,66] reaffirmed that the change in the width of the tunneling barrier is more important than the change in the barrier height. It is tempting to say that an explanation was given for the observed decrease in the tunneling splitting, but 2-D constrained variational results, when the potential is not allowed to relax along the constrained modes, yield the opposite answer,[36] showing how subtle this effect is.

The $2\nu_2$ overtone is still under the barrier, but just barely, the upper (a) energy level is at 1882.1784(12) cm^{-1}. The splitting is thus much enhanced, as expected, it is about 284.6 cm^{-1} compared to 35.7 cm^{-1} for ν_2.

The situation is different for the E-type stretching and bending motions. Within the $\nu_2 + \nu_3$ mode the splitting is quenched even more effectively, from 35.7 to 18.5314(22) cm^{-1}. As to $\nu_2 + \nu_4$, the splitting is enhanced, from 35.7 to 45.6031(24) cm^{-1}. Thus, seemingly either a symmetric or an antisymmetric stretching of the N–H bonds decreases the splittings, while the antisymmetric bending enhances the splitting, in other words it decreases the effective barrier height or decreases the effective length of the tunneling path.

The tunneling splittings characterizing the VBOs in which the umbrella motion is not involved are on the order of 1 cm^{-1}, similar to the splitting of the "ground" vibrational state. For example, the vibrational tunneling splittings are 1.4354(36) cm^{-1} for $2\nu_4^2$, 0.9315(32) cm^{-1} for $\nu_1 + \nu_3^1$, 0.8787(28) cm^{-1} for $\nu_3 + 2\nu_4^2$, and 0.4101(66) cm^{-1} for $2\nu_3^2$, where the value of $|L|$ is given in the superscript for the degenerate modes. Once again, stretching motions seem to quench, while bending motions seem to enhance the vibrational tunneling splittings. Though the trend is not very clear, it is clear that the effect is relatively minor. Unfortunately, no experimental data are available to study further the promotion or inhibition of vibrational tunneling splittings of $^{14}NH_3$. Analysis of the first-principles BYTe data[51] shows that the maximum splitting up to 10 000 cm^{-1} stays below about 10 cm^{-1} for states not involving the ν_2 bending motion, supporting the above conclusion.
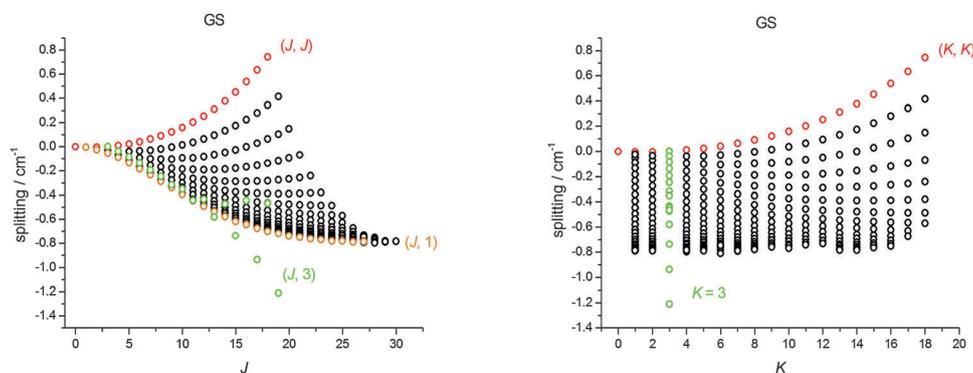

Fig. 2 Energy differences E(a) − E(s), as a function of the J (left figure) and the K (right figure) quantum numbers, of all the corresponding rotational levels on the 0^+ and 0^- vibrational states present in the MARVEL database[36] of $^{14}NH_3$.

This journal is © the Owner Societies 2016

Phys. Chem. Chem. Phys., 2016, 18, 1092–1104 | 1095

4 The effect of rotation on tunneling splittings

In the following we consider qualitatively what happens with the tunneling splittings when the J and K rotational quantum numbers assume larger and larger values. The discussion is supported by several figures and it is given separately for the vibrational bands. Fig. 2–10 show energy differences $E(a) - E(s)$ as a function of the J and K quantum numbers for 20 VBOs, for which a sufficiently large set of MARVEL rovibrational energy levels is available. The order of the figures basically follows the order of the fundamentals. In all figures, where appropriate, the limiting (J,J) and $(J,1)$, occasionally $(J,0)$, splittings are color coded by red and orange, respectively, while the unorthodox $(J,3)$, occasionally $(J,2)$, cases are given in green to increase the information content of the figures.

First, discuss the rotational states $(J,K) = (J,J)$. For these states the rotational angular momentum is "parallel" to the main symmetry axis and thus K has its maximum value. The corresponding rotation flattens the molecule and the centrifugal distortion increases the N–H distances simultaneously leading to an increased H–H distance. The overall effect is an increase in the tunneling splitting. The expectation is that the tunneling splitting increases fast as J in (J, J) increases. This can be observed very clearly not only for the "ground" state (Fig. 2), but also for the ν_2 (the lower row of Fig. 5), $2\nu_2$, and $3\nu_2$ (Fig. 8) vibrational states. Fig. 3 shows the effect for the vibrational states 0^+ and 0^- in the case of the first-principles BYTe[51] energy levels, for which higher K values are available. The increase turns out to be clearly quadratic in K. A similar observation can be made for the $(J,J - 1)$ levels. However, starting perhaps for the rotational states of about $(J,J - 4)$ and for even lower K values, the simple quadratic dependence changes and the tunneling splittings do not change in a simple increasing or decreasing fashion though the changes remain highly regular.

For non-degenerate VBOs, e.g., the ground state (GS), but also for ν_1 and ν_2, the other limiting case corresponds to the

Fig. 4 Comparison of the experimental MARVEL,[36] red circles, and the first-principles BYTe,[51] blue circles, tunneling splittings for $K = 1$ (top figure), $K = 3$ (middle figure), and $K = 6$ (bottom figure) as a function of the J rotational quantum number for all the rotational levels on the 0^+ and 0^- vibrational states of $^{14}NH_3$.
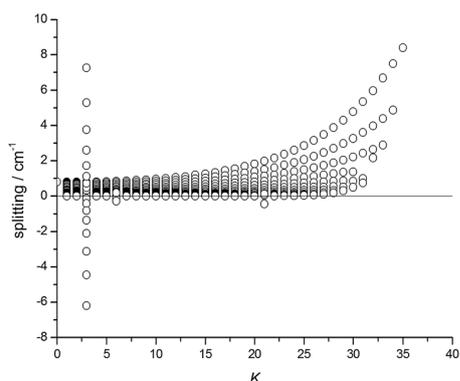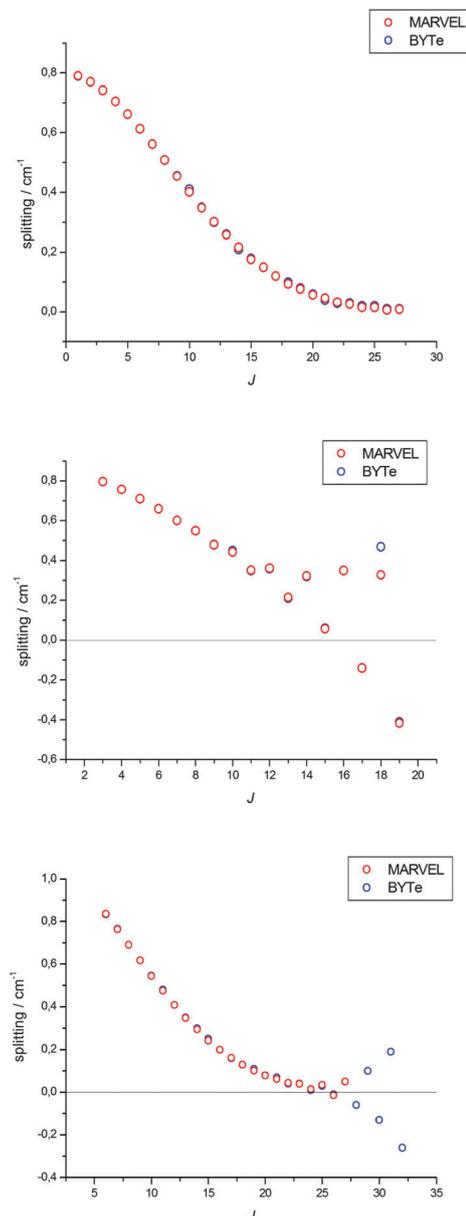

Fig. 3 Energy differences $E(a) - E(s)$, as a function of the K quantum number, of all the corresponding rotational levels on the 0^+ and 0^- vibrational states present in the first-principles BYTe list[51] of $^{14}NH_3$, showing considerable deviations from the regular pattern for $K = 3$.

$(J,K) = (J,1)$ energy levels, as the $K = 0$ states are missing due to symmetry. In this case the rotational axis is "perpendicular" to the main symmetry axis. The rotational motion tends to increase the NX distance, where X is the middle point of the three Hs, and thus the height of the inversion barrier and decrease the H–H distance. The change in the shape of the inversion barrier leads to a decreased tunneling splitting. For the "ground" vibrational state (see Fig. 2), for which MARVEL data provide the most complete coverage, it seems that the effective height of the tunneling barrier becomes so high (or the effective tunneling path length so short) by $J = 25$
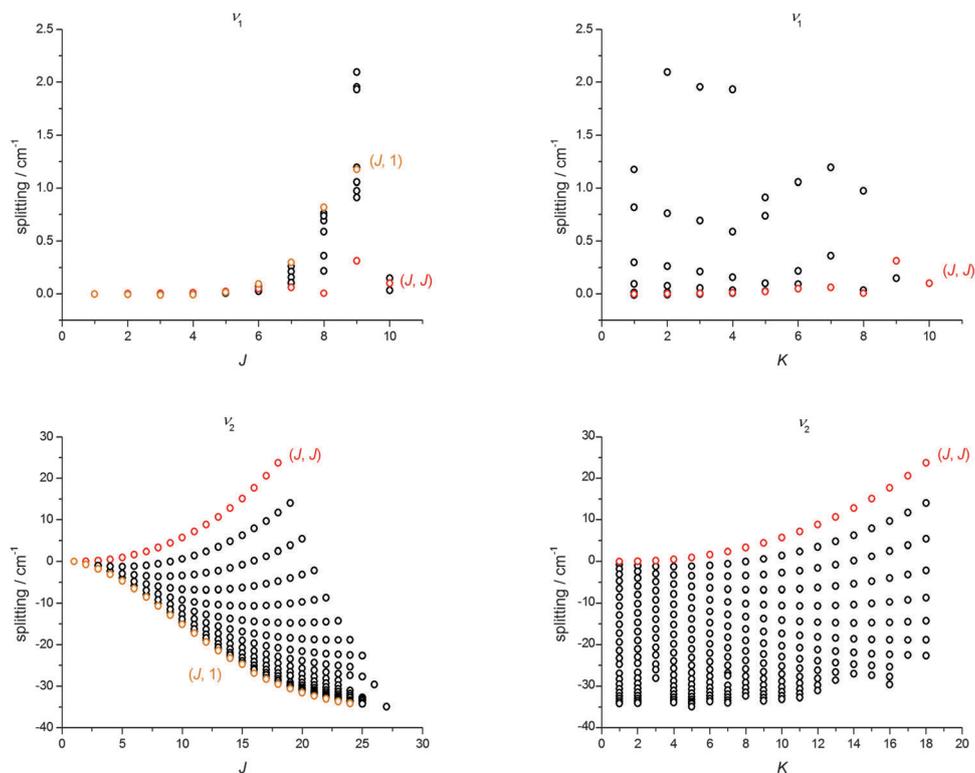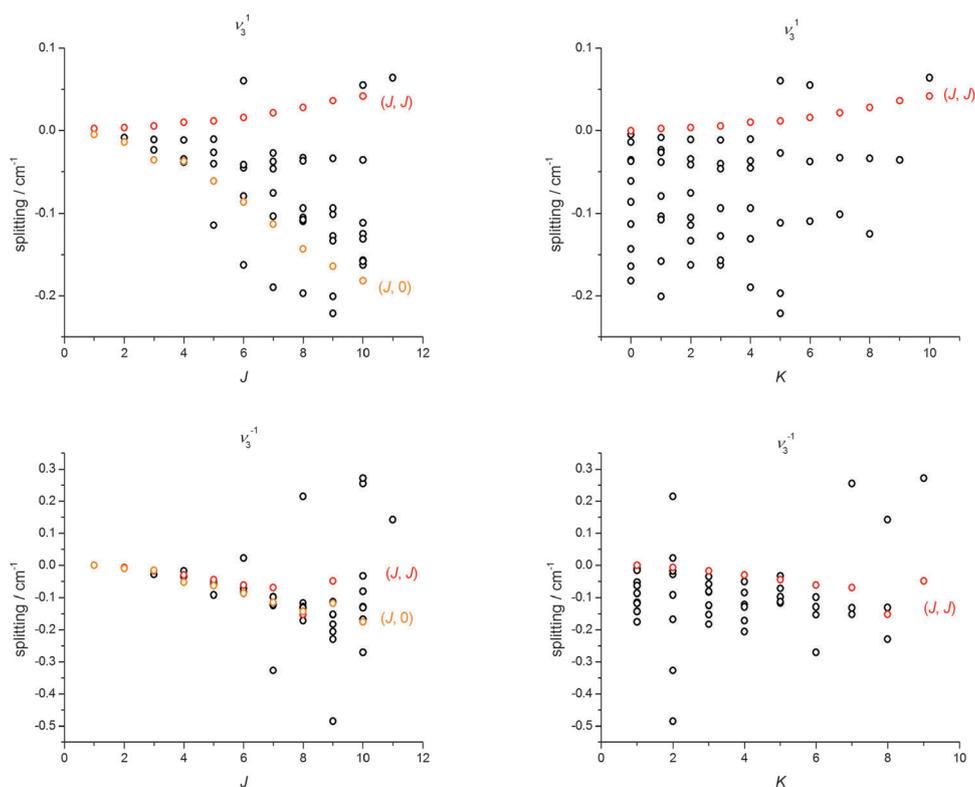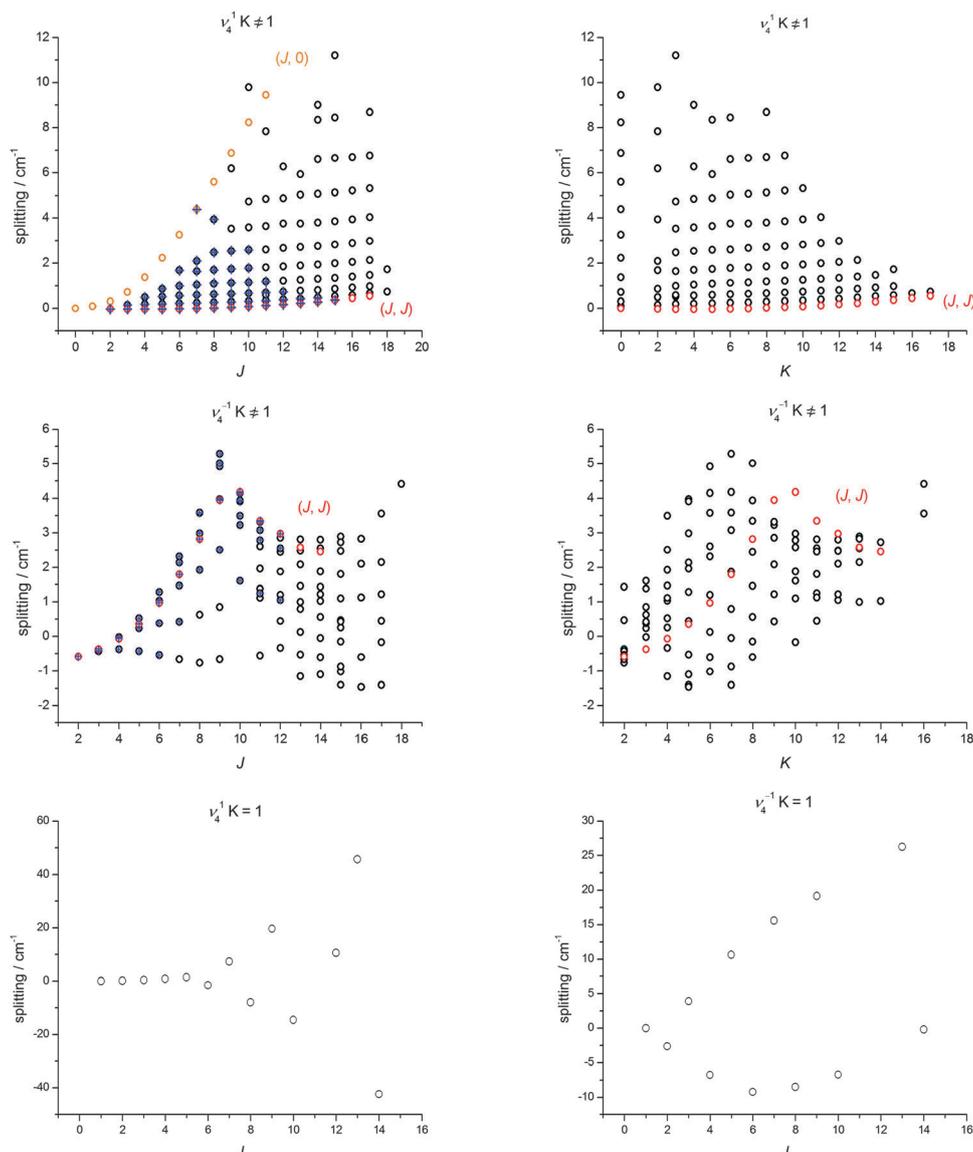
Fig. 5 Energy differences $E(a) - E(s)$, as a function of the J (left-hand figures) and the K (right-hand figures) quantum numbers, of all the corresponding rotational levels on the nondegenerate vibrational fundamentals present in the MARVEL database[36] of $^{14}NH_3$: ν_1^+ and ν_1^- (first row) and ν_2^+ and ν_2^- (second row).

Fig. 6 Energy differences $E(a) - E(s)$, as a function of the J (left-hand figures) and the K (right-hand figures) quantum numbers, of all the corresponding rotational levels on the degenerate vibrational fundamental ν_3^+ and ν_3^- present in the MARVEL database[36] of $^{14}NH_3$.

This journal is © the Owner Societies 2016

Phys. Chem. Chem. Phys., 2016, 18, 1092–1104 | 1097

Fig. 7 In the upper two rows, energy differences $E(a) - E(s)$ are given as a function of the J (left-hand figures) and the K (right-hand figures) quantum numbers of all the corresponding rotational levels but $K = 1$ on the degenerate vibrational fundamental ν_4^+ and ν_4^- present in the MARVEL database[36] of $^{14}NH_3$. The blue crosses of the J-dependent plots correspond to experimentally measured transitions published in ref. 57 and 68–70. The $K = 1$ tunneling splittings are given in the third row.

that the split s and a rotational states start to become degenerate; thus, the splittings between them approach zero. This finding is confirmed by the BYTe data[51] extending to higher J values, as seen clearly in the top panel of Fig. 4.

When $K \neq 3n$, $n = 0, 1, 2,\ldots$, the doubly degenerate rotational levels belong to $E^{\dagger}$ and cannot be split apart by perturbations possessing a threefold symmetry.[67] Transitions among these energy levels show a regular pattern straightforward to the model (Fig. 2). When $K = 3n$, $n = 1, 2,\ldots$, the two levels belong to two distinct irreps, $A_1^{\dagger}$ and $A_2^{\dagger}$. The levels become separated by a threefold-degenerate perturbation. As discussed above, of the two components the $A_1^{\dagger}$ one is 'missing'.

The "normal" behavior of the rotational tunneling splitting differences on the 0^+ and 0^- split vibrational ground states is

seen in the top panel of Fig. 4, where the $K = 1$ behavior is shown as a function of the J rotational quantum number based not only on MARVEL but also on the more extended BYTe list. While Simmons and Gordy[35] observed in 1948 "no apparent shift from a smooth curve of lines for which $K = 6$ or higher multiples of 3", the more complete MARVEL and BYTe data reveal shifts for higher J values both for $K = 3$ and 6, see Fig. 4. Comparison of the $K = 3$ and $K = 6$ results shows that the anomalous behavior starts at a considerably higher J value in the case of $K = 6$. It must also be emphasized that on the scale of Fig. 4 the MARVEL and BYTe results, when both are available, show agreement; thus, the qualitative trends are well established experimentally and confirmed theoretically.
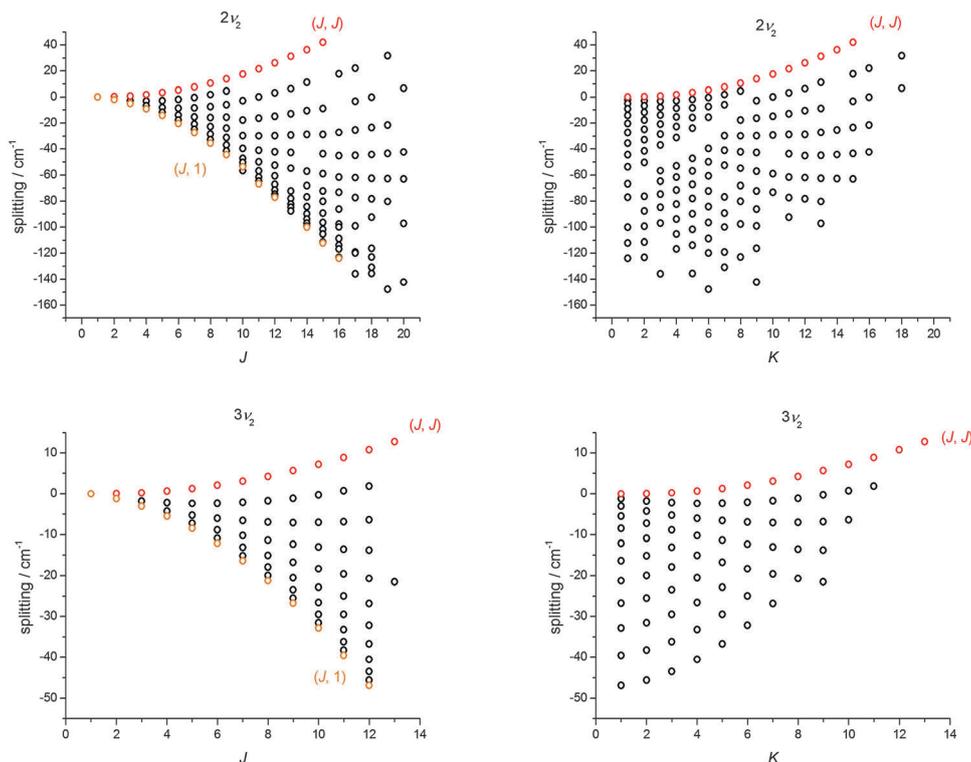
Fig. 8 Energy differences $E(a) - E(s)$, as a function of the J (left-hand figures) and the K (right-hand figures) quantum numbers, of all the corresponding rotational levels on the $2\nu_2^+$ and $2\nu_2^-$ (first row), and $3\nu_2^+$ and $3\nu_2^-$ (second row) vibrations in the MARVEL database[36] of $^{14}NH_3$.

While the number of measured splittings is relatively small for the ν_1 fundamental (see the first row of Fig. 5), some tendencies can still be observed, though others may remain hidden. All the observed splittings remain small, on the order of 1 cm^{-1}, whereby the purely vibrational splitting is 1.0 cm^{-1} (Fig. 1). There are no negative splitting values in Fig. 1, suggesting that the rotation, when coupled to the symmetric stretch motion, allows for more efficient tunneling. Furthermore, the splittings seem to increase as J increases.

As to coupling of rotation to the ν_3 motion (Fig. 6), recall that the pure vibrational splitting is 0.3596(14) cm^{-1}, the smallest of the set containing the GS and the fundamentals of $^{14}NH_3$. The limited amount of experimental information suggests that for low J values the splitting remains small, no splitting larger than 0.5 cm^{-1} has been observed. A couple of clear tendencies can be observed in Fig. 6, especially for the $l_3 = +1$ case (see first row of Fig. 6). It is also clear that due to the $k - l = 3n$ rule[36] the $K = 2$ case is special for ν_3, the splittings are again considerably larger and divergent as compared to other K values. The largest observed splittings correspond to the [7 2 i] and [9 2 i] cases. It is also notable that the effect of rotation on the splittings can be both positive and negative; $i.e.$, rotation can both promote and inhibit the underlying vibrational splitting.

Splittings characterizing the ν_4 fundamental are depicted in Fig. 7. In order not to destroy the scale of the figure, the splittings corresponding to $K = 1$ are separated from the rest of the data and are depicted in the third row of Fig. 7. The $l_4 = +1$ splittings are all positive and increase substantially as

J increases, by $J = 15$ the splitting increases to almost 20 cm^{-1} from the vibration-only splitting of 1.0977(27) cm^{-1}. The $l_4 = -1$ splittings exhibit much less well defined characteristics, likely due to the limited amount of information available. As to the $K = 1$ splittings, the $l_4 = +1$ and $l_4 = -1$ points show a somewhat different behavior but in both cases the splittings diverge as J increases, though they remain close to zero up to about $J = 6$. Proper empirical modeling of this behavior may present considerable difficulties.

The $\nu_1 + \nu_3^1$ data in the first row of Fig. 9 show considerable scatter and no obvious trends. This is mostly due to the small number of data points available. In clear contrast, the data for the $\nu_2 + \nu_3^1$ and $\nu_2 + \nu_4^1$ combination bands show well-defined characteristics, though the small number of available points hinders making definitive conclusions. The special nature of the $K = 1$, 4 and 7 splittings is clearly visible in the $\nu_2 + \nu_3^1$ and $\nu_2 + \nu_4^1$ cases.

Fig. 10 not only provides a detailed view on tunneling splitting trends characterizing the first overtone of the fundamental ν_4, $2\nu_4$, but it also allows for a comparison between MARVEL splitting results and those of Huang et $al.$,[52] representing high-quality first-principles predictions. In fact, Fig. 10 was prepared to allow a direct comparison with Fig. 1 of ref. 52. Clearly, for the $2\nu_4^2$ levels ($J = 0$–7) the experimental MARVEL,[36] the mixed experimental and theoretical HITRAN,[71] and the first-principles HSL-2[52] data show perfect agreement. Another observation is that the K-dependent splitting "curves" show considerable scatter for some of the J values, suggesting the

This journal is © the Owner Societies 2016

Phys. Chem. Chem. Phys., 2016, **18**, 1092–1104 | **1099**
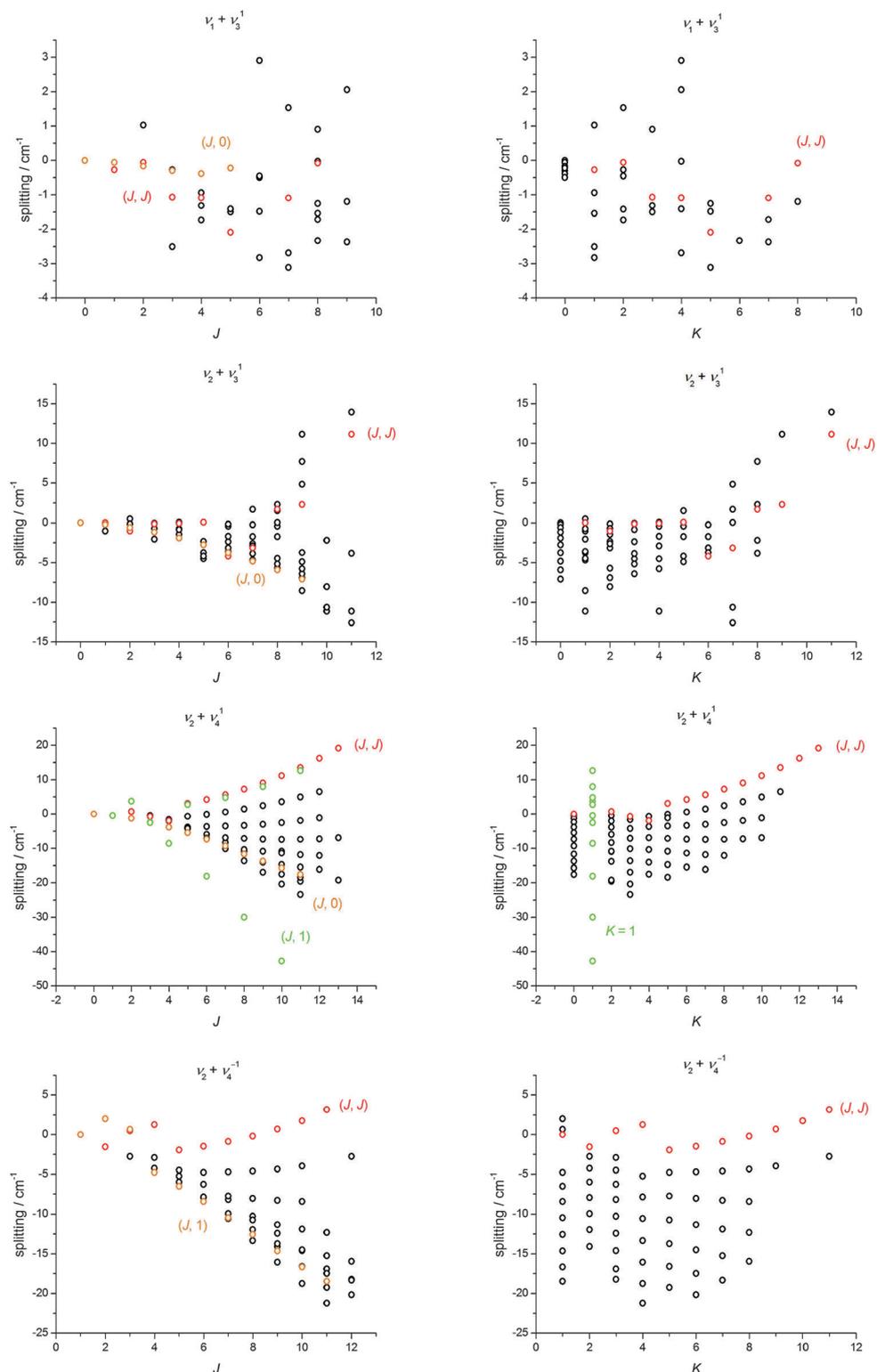
Fig. 9 Energy differences $E(a) - E(s)$, as a function of the J (left-hand figures) and the K (right-hand figures) quantum numbers, of all the corresponding rotational levels on the $(\nu_1 + \nu_3)^+$ and $(\nu_1 + \nu_3)^-$ (first row), $(\nu_2 + \nu_3)^+$ and $(\nu_2 + \nu_3)^-$ (second row), and $(\nu_2 + \nu_4)^+$ and $(\nu_2 + \nu_4)^-$ (third and fourth rows) combination bands in the MARVEL database[36] of $^{14}NH_3$.

presence of strong resonances. For the other two l values the MARVEL tunneling splittings always agree with their HSL-2 counterparts and confirm the somewhat irregular behavior

pointed out in ref. 52. It seems quite likely that for even higher-energy vibrations the assignment of experimental spectra must rely on MARVEL-type ''experimental'' energy
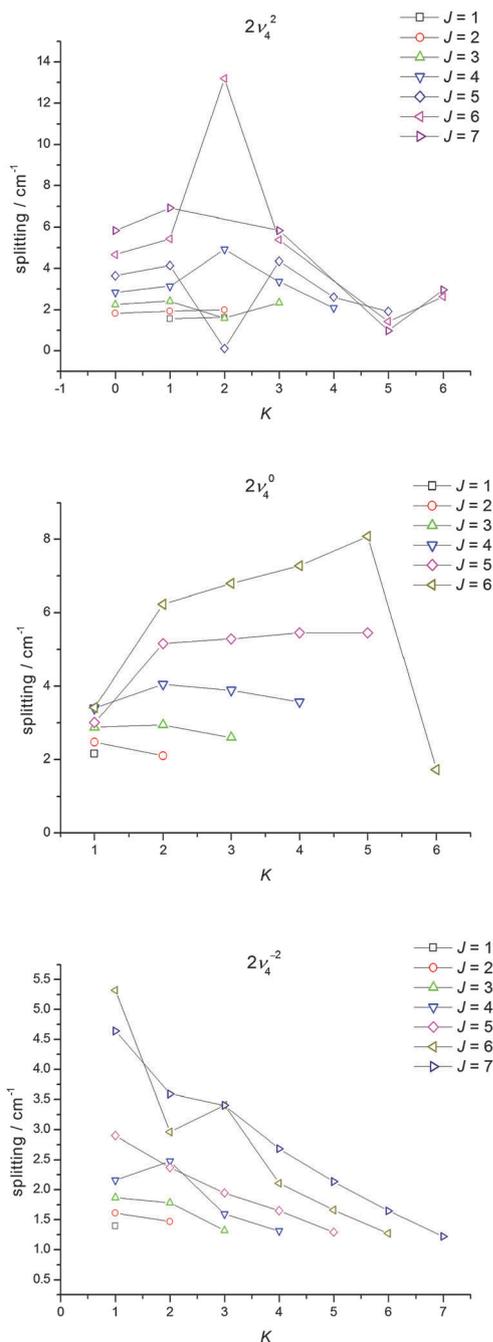
Fig. 10 Detailed and color-coded plot of the energy differences E(a) − E(s) on the $2\nu_4^{+2}$, $2\nu_4^0$, and $2\nu_4^{-2}$ overtone bands in the MARVEL database[36] of $^{14}NH_3$.

levels augmented with their accurate first-principles nuclear motion counterparts.

5 Summary and conclusions

There is an increased realization[56,66] that tunneling is important for several classes of chemical reactions. It is our belief that the model symmetric double-well problem characterizing

the tunneling motion of ammonia contributes to our understanding how chemical reactions can be promoted or inhibited through nuclear motions, $i.e.$, through state-selective excitations. The reason that tunneling is an ideal candidate to investigate the related dynamics is that state-dependent tunneling splittings are extremely sensitive to even small changes in the shape of the effective barriers hindering tunneling.

The complexity of the high-resolution spectra of $^{14}NH_3$, emphasized already by Herzberg,[72] is due to several reasons. One is the high symmetry of the molecule resulting in "unusual" restrictions for the energy levels and the transitions and a large number of perturbations. Another one is the characteristic tunneling motion in a symmetric double-well potential. As shown in this study, the energy-resolved characterization of the complex nuclear motions of $^{14}NH_3$ contributes not only to our improved appreciation of molecular spectroscopy but also to the understanding of chemical reactions and the effect of nuclear motions on them. The experimental tunneling splittings characterizing the rovibrational states of $^{14}NH_3$ have been investigated and rationalized here with the following important findings.

As expected, the umbrella motion is unique among the vibrational motions of $^{14}NH_3$ in that it greatly promotes tunneling. The other pure vibrational motions have only a minor effect on the tunneling splitting of the corresponding antisymmetric and symmetric states. Either symmetric or antisymmetric stretching decreases the splittings, which can be rationalized by a corresponding increase in the tunneling path length. Antisymmetric bending promotes tunneling but to a much smaller extent than its symmetric counterpart.

For rotational states $(J,K) = (J,J)$, $i.e.$, for "parallel" rotations, the tunneling splitting increases quadratically as J increases. The effect is especially pronounced for the $n\nu_2$, $n = 1, 2,\ldots$, states. Thus, parallel rotation promotes tunneling. The splitting characterizing the ν_2 fundamental is 35.7 cm^{-1}, a similar "extra" splitting, yet unobserved, is reached by about $J = 25$, a substantial but perfectly feasible rotational excitation.

The other limiting case for rotations concerns the $(J,K) = (J,1)$ states, as for non-degenerate VBOs the $K = 0$ states are missing for symmetry reasons. This "perpendicular" rotation motion inhibits tunneling. This inhibition is so effective that, for example, for the ground vibrational state the splitting decreases basically to zero by about $J = 25$.

The rule $k − l = 3n$ is responsible for a large number of irregular splittings characterizing the nuclear motion of $^{14}NH_3$. For these special cases the splittings are considerably larger and show a divergent trend, allowing for an interesting dynamical behavior challenging to understand. Another characteristics is that the splittings can both be positive and negative; thus, these special rotations can both promote and inhibit the underlying vibrational splittings.

In the limited number of cases checked, the findings of the present study about tunneling splitting trends characterizing different rovibrational cases are fully supported by first-principles data. The quantum chemical results also allow for extensions of the experimental findings and should prove to be highly useful for a more detailed understanding of the complex

This journal is © the Owner Societies 2016

Phys. Chem. Chem. Phys., 2016, **18**, 1092–1104 | **1101**

spectra and molecular motions of $^{14}NH_3$. The present results also contribute to our deeper understanding of reaction control *via* nuclear motions.

Acknowledgements

References

1 W. W. Coblentz, Infra-red absorption spectra, II. Liquids and solids, *Phys. Rev.*, 1905, **20**, 337–363.

2 K. Schierkolk, Das ultrarote Absorptionsspektrum des Ammoniaks, *Z. Phys.*, 1924, **29**, 277–287.

3 D. M. Dennison, On the analysis of certain molecular spectra, *Philos. Mag.*, 1926, **1**, 195–218.

4 R. Robertson, J. J. Fox and E. S. Hiscocks, Studies in the infra-red region of the spectrum. Part II. Calibration of prism spectrometer; general procedure; and preparation of pure ammonia, phosphine and arsine, *Proc. R. Soc. London, Ser. A*, 1928, **120**, 149–160.

5 R. Robertson and J. J. Fox, Studies in the infra-red region of the spectrum. Part III. Infra-red absorption spectra of ammonia, phosphine and arsine, *Proc. R. Soc. London, Ser. A*, 1928, **120**, 161–189.

6 R. Robertson and J. J. Fox, Studies in the infra-red region of the spectrum. Part IV. Discussion of absorption bands of ammonia, phosphine and arsine, *Proc. R. Soc. London, Ser. A*, 1928, **120**, 189–210.

7 R. M. Badger and C. H. Cartwright, The pure rotation spectrum of ammonia, *Phys. Rev.*, 1929, **33**, 692–700.

8 E. F. Barker, The molecular spectrum of ammonia. II. The double band at 10 μ, *Phys. Rev.*, 1929, **33**, 684–691.

9 R. G. Dickson, R. T. Dillon and F. Rasetti, Raman spectra of polyatomic gases, *Phys. Rev.*, 1929, **34**, 582–589.

10 G. A. Stinchcomb and E. F. Barker, The molecular spectrum of ammonia. I. Two types of infra-red vibration bands, *Phys. Rev.*, 1929, **33**, 305–308.

11 R. W. Wood, The Raman effect in gases. – Part I. HCl and NH₃, *Philos. Mag.*, 1929, **7**, 744.

12 D. M. Dennison, The infrared spectra of polyatomic molecules. Part I, *Rev. Mod. Phys.*, 1931, **3**, 280–345.

13 D. M. Dennison and J. D. Hardy, The parallel type absorption bands of ammonia, *Phys. Rev.*, 1932, **39**, 938–947.

14 D. M. Dennison and G. E. Uhlenbeck, The two-minima problem and the ammonia molecule, *Phys. Rev.*, 1932, **41**, 313–321.

15 E. Fermi, Sulle bande di oscillazione e rotazione dell'ammoniaca, *Nuovo Cimento*, 1932, **9**, 277–283.

16 H. J. Unger, Infrared absorption bands of ammonia, *Phys. Rev.*, 1933, **43**, 123–128.

17 N. Wright and H. M. Randall, The far infrared spectra of ammonia and phosphine gases under high resolving power, *Phys. Rev.*, 1933, **44**, 391–398.

18 C. E. Cleeton and N. H. Williams, Electromagnetic waves of 1.1 cm wave-length and the absorption spectrum of ammonia, *Phys. Rev.*, 1934, **45**, 234–237.

19 R. B. Barnes, The pure rotation spectra of NH₃ and ND₃, *Phys. Rev.*, 1935, **47**, 658–661.

20 S.-H. Chao, The photographic absorption spectrum of gaseous ammonia, *Phys. Rev.*, 1935, **48**, 569.

21 M. F. Manning, Energy levels of a symmetrical double minima problem with applications to the NH₃ and ND₃ molecules, *J. Chem. Phys.*, 1935, **3**, 136–138.

22 E. F. Barker, Perpendicular vibrations of the ammonia molecule, *Phys. Rev.*, 1939, **55**, 657–662.

23 Z. I. Slawsky and D. M. Dennison, The centrifugal distortion of axial molecules, *J. Chem. Phys.*, 1939, **7**, 509–521.

24 D. M. Dennison, The infra-red spectra of polyatomic molecules. Part II, *Rev. Mod. Phys.*, 1940, **12**, 175–214.

25 H.-Y. Sheng, E. F. Barker and D. M. Dennison, Further resolution of two parallel bands of ammonia and the interaction between vibration and rotation, *Phys. Rev.*, 1941, **60**, 786–794.

26 B. Bleaney and R. P. Penrose, Ammonia spectrum in the 1 cm. wave-length region, *Nature*, 1946, **157**, 339–340.

27 W. E. Good, The inversion spectrum of ammonia, *Phys. Rev.*, 1946, **70**, 213–218.

28 B. Bleaney and R. P. Penrose, The inversion spectrum of ammonia at centimetre wave-lengths, *Proc. R. Soc. London, Ser. A*, 1947, **189**, 358–371.

29 W. E. Good and D. K. Coles, Microwave absorption frequencies of $^{14}NH_3$ and $^{15}NH_3$, *Phys. Rev.*, 1947, **72**, 383–384.

30 W. Gordy and M. Kessler, Microwave spectra: The hyperfine structure of ammonia, *Phys. Rev.*, 1947, **71**, 640.

31 H. H. Nielsen and D. M. Dennison, Anomalous values of certain of the fine structure lines in the ammonia microwave spectrum, *Phys. Rev.*, 1947, **72**, 1101–1108.

32 M. W. P. Strandberg, R. Kyhl, T. Wentink Jr and R. E. Hillger, Inversion spectrum of ammonia, *Phys. Rev.*, 1947, **71**, 326.

33 M. W. P. Strandberg, R. Kyhl, T. Wentink Jr and R. E. Hillger, Inversion spectrum of ammonia, *Phys. Rev.*, 1947, **71**, 639.

34 R. J. Watts and D. Williams, Nuclear quadrupole moment effects in the microwave spectrum of ammonia, *Phys. Rev.*, 1947, **72**, 639.

35 J. W. Simmons and W. Gordy, Structure of the inversion spectrum of ammonia, *Phys. Rev.*, 1948, **73**, 713–718.

36 A. R. Al Derzi, T. Furtenbacher, J. Tennyson, S. N. Yurchenko and A. G. Császár, MARVEL analysis of the measured high-resolution spectra of $^{14}NH_3$, *J. Quant. Spectrosc. Radiat. Transfer*, 2015, **116**, 117–130.

37 E. Kauppi and L. Halonen, Five-dimensional local mode-Fermi resonance model for overtone spectra of ammonia, *J. Chem. Phys.*, 1995, **103**, 6861–6872.

38 W. Klopper, C. C. M. Samson, G. Tarczay and A. G. Császár, Equilibrium inversion barrier of NH₃ from extrapolated

coupled-cluster pair energies, *J. Comput. Chem.*, 2001, **22**, 1306–1314.

39 T. Rajamäki, M. Kállay, T. Noga, P. Valiron and L. Halonen, High excitations in coupled-cluster series: Vibrational energy levels of ammonia, *Mol. Phys.*, 2004, **102**, 2297–2310.

40 C. Puzzarini, Ab initio characterization of XH₃ (X = N, P). Part II. Electric, magnetic and spectroscopic properties of ammonia and phosphine, *Theor. Chem. Acc.*, 2008, **121**, 1–10.

41 A. G. Császár, W. D. Allen and H. F. Schaefer III, In pursuit of the *ab initio* limit for conformational energy prototypes, *J. Chem. Phys.*, 1998, **108**, 9751–9764.

42 J. P. Gordon, H. J. Zeiger and C. H. Townes, Molecular microwave oscillator and new hyperfine structure in the microwave spectrum of NH₃, *Phys. Rev.*, 1954, **95**, 282–284.

43 A. G. Császár, G. Tarczay, M. L. Leininger, O. L. Polyansky, J. Tennyson and W. D. Allen, in *Dream or reality: complete basis set full configuration interaction potential energy hypersurfaces*, ed. J. Demaison and K. Sarka, Spectroscopy from Space, Kluwer, 2001, pp. 317–339.

44 R. Marquardt, K. Sagui, J. Zheng, W. Thiel, D. Luckhaus, S. Yurchenko, F. Mariotti and M. Quack, Global analytical potential energy surface for the electronic ground state of NH₃ from high level *ab initio* calculations, *J. Phys. Chem. A*, 2013, **117**, 7502–7522.

45 A. G. Császár, C. Fábri, T. Szidarovszky, E. Mátyus, T. Furtenbacher and G. Czakó, Fourth age of quantum chemistry: Molecules in motion, *Phys. Chem. Chem. Phys.*, 2012, **14**, 1085–1106.

46 E. Mátyus, G. Czakó, B. Sutcliffe and A. G. Császár, Variational vibrational calculations with arbitrary potentials using the Eckart--Watson Hamiltonians and the discrete variable representation, *J. Chem. Phys.*, 2007, **127**, 084102.

47 S. N. Yurchenko, W. Thiel and P. Jensen, Theoretical ROVibrational energies (TROVE): A robust numerical approach to the calculation of rovibrational energies for polyatomic molecules, *J. Mol. Spectrosc.*, 2007, **245**, 126–140.

48 E. Mátyus, J. iimunek and A. G. Császár, On variational computation of a large number of vibrational energy levels and wave functions for medium-sized molecules, *J. Chem. Phys.*, 2009, **131**, 074106.

49 E. Mátyus, G. Czakó and A. G. Császár, Toward black-box-type full- and reduced-dimensional variational (ro)vibrational computations, *J. Chem. Phys.*, 2009, **130**, 134112.

50 C. Fábri, E. Mátyus and A. G. Császár, Rotating full- and reduced-dimensional quantum chemical models of molecules, *J. Chem. Phys.*, 2011, **134**, 074105.

51 S. N. Yurchenko, R. J. Barber and J. Tennyson, A variationally computed hot line list for NH₃, *Mon. Not. R. Astron. Soc.*, 2011, **413**, 1828–1834.

52 X. Huang, D. W. Schwenke and T. J. Lee, Rovibrational spectra of ammonia. II. Detailed analysis, comparison, and prediction of spectroscopic assignments for ¹⁴NH₃¹⁵NH₃, and ¹⁴ND₃, *J. Chem. Phys.*, 2011, **134**, 044321.

53 M. Snels, L. Fusina, H. Hollenstein and M. Quack, The ν_1 and ν_3 bands of ND₃, *Mol. Phys.*, 2000, **98**, 837–854.

54 M. Snels, H. Hollenstein and M. Quack, The NH and ND stretching fundamentals of ¹⁴ND₂H, *J. Chem. Phys.*, 2003, **119**, 7893–7901.

55 M. Snels, H. Hollenstein and M. Quack, The NH and ND stretching fundamentals of ¹⁴NH₂D, *J. Mol. Spectrosc.*, 2006, **237**, 143–148.

56 R. P. Bell, *The Tunnel Effect in Chemistry*, Chapman and Hall, London, 1980.

57 E. A. Cohen, The ν_4 state inversion spectra of ¹⁵NH₃ and ¹⁴NH₃, *J. Mol. Spectrosc.*, 1980, **79**, 496–501.

58 A. G. Császár, G. Czakó, T. Furtenbacher and E. Mátyus, An active database approach to complete spectra of small molecules, *Annu. Rep. Comput. Chem.*, 2007, **3**, 155–176.

59 A. G. Császár and T. Furtenbacher, Spectroscopic networks, *J. Mol. Spectrosc.*, 2011, **266**, 99–103.

60 T. Furtenbacher, A. G. Császár and J. Tennyson, MARVEL: measured active rotational-vibrational energy levels, *J. Mol. Spectrosc.*, 2007, **245**, 115–125.

61 T. Furtenbacher and A. G. Császár, On employing H₂¹⁶O, H₂¹⁷O, H₂¹⁸O, and D₂¹⁶O lines as frequency standards in the 15–170 cm⁻¹ window, *J. Quant. Spectrosc. Radiat. Transfer*, 2008, **109**, 1234–1251.

62 T. Furtenbacher and A. G. Császár, MARVEL: measured active rotational-vibrational energy levels. II. Algorithmic improvements, *J. Quant. Spectrosc. Radiat. Transfer*, 2012, **113**, 929–935.

63 P. R. Bunker and P. Jensen, *Molecular Symmetry and Spectroscopy*, NRC Research, 1998.

64 M. J. Down, C. Hill, S. N. Yurchenko, J. Tennyson, L. R. Brown and I. Kleiner, Re-analysis of ammonia spectra: Updating the HITRAN ¹⁴NH₃ database, *J. Quant. Spectrosc. Radiat. Transfer*, 2013, **130**, 260–272.

65 P. R. Schreiner, H. P. Reisenauer, F. C. Pickard, A. C. Simmonett, W. D. Allen, E. Mátyus and A. G. Császár, Capture of hydroxymethylene and its fast disappearance through tunnelling, *Nature*, 2008, **453**, 906–909.

66 D. Ley, D. Gerbig and P. R. Schreiner, Tunnelling control of chemical reactions – the organic chemists perspective, *Org. Biomol. Chem.*, 2012, **10**, 3781–3790.

67 H. H. Nielsen and D. M. Dennison, Anomalous values of certain of the fine structure lines in the ammonia microwave spectrum, *Phys. Rev.*, 1947, **72**, 86–87.

68 H. Sasada, Y. Endo, E. Hirota, R. L. Poynter and J. S. Margolis, Microwave and Fourier-transform infrared spectroscopy of the $\nu_4 = 1$ and $\nu_2 = 2$ states of NH₃, *J. Mol. Spectrosc.*, 1992, **151**, 33–53.

69 E. A. Cohen and R. L. Poynter, The microwave spectrum of ¹⁴NH₃ in the $\nu = 000011$ state, *J. Mol. Spectrosc.*, 1974, **53**, 131–139.

70 H. Sasada, Y. Hasegawa, T. Amano and T. Shimizu, High-resolution infrared and microwave spectroscopy of the ν_4 and $2\nu_2$ bands of ¹⁴NH₃ and ¹⁵NH₃, *J. Mol. Spectrosc.*, 1982, **96**, 106–130.

71 L. S. Rothman, I. E. Gordon, A. Barbe, D. C. Benner, P. F. Bernath, M. Birk, V. Boudon, L. R. Brown, A. Campargue, J. P. Champion, K. Chance, L. H. Coudert, V. Dana, V. M. Devi, S. Fally, J. M. Flaud, R. R. Gamache,

This journal is © the Owner Societies 2016

Phys. Chem. Chem. Phys., 2016, **18**, 1092–1104 | **1103**

A. Goldman, D. Jacquemart, I. Kleiner, N. Lacome, W. J. Lafferty, J. Y. Mandin, S. T. Massie, S. N. Mikhailenko, C. E. Miller, N. Moazzen-Ahmadi, O. V. Naumenko, A. V. Nikitin, J. Orphal, V. I. Perevalov, A. Perrin, A. Predoi-Cross, C. P. Rinsland, M. Rotger, M. Simeckova, M. A. H. Smith, K. Sung, S. A. Tashkun, J. Tennyson, R. A. Toth, A. C. Vandaele and J. Vander Auwera, The HITRAN 2008 molecular spectroscopic database, *J. Quant. Spectrosc. Radiat. Transfer*, 2009, **110**, 533–572.

72 G. Herzberg, *Molecular spectra and molecular structure*, Van Nostrand Reinhold, Melbourne, 1945, vol. 1–3.